Journal of Anatomy

J. Anat. (2018) **233**, pp740–754 doi: 10.1111/joa.12886

Exploring bone volume and skeletal weight in the Middle Pleistocene humans from the Sima de los Huesos site (Sierra de Atapuerca, Spain)

José-Miguel Carretero,[1,2] Laura Rodríguez,[1] Rebeca García-González,[1] Rolf-Michael Quam[2,3,4] and Juan-Luis Arsuaga[2,5]

[1]*Laboratorio de Evolución Humana, Universidad de Burgos, Edificio I+D+i, Burgos, Spain*
[2]*Centro UCM-ISCIII de Investigación sobre Evolución y Comportamiento Humanos, Madrid, Spain*
[3]*Department of Anthropology, Binghamton University (SUNY), Binghamton, New York, USA*
[4]*Division of Anthropology, American Museum of Natural History, New York, New York, USA*
[5]*Facultad de Ciencias Geológicas, Departamento de Paleontología, Universidad Complutense de Madrid, Madrid, Spain*

Abstract

Body mass estimation in fossil human species is a crucial topic in paleoanthropology as it yields information about ecologically relevant characteristics. Nevertheless, variables crucial to body mass estimation such as bone volume and skeletal weight have never before been calculated in a fossil human species. The exceptional state of preservation of several fossil human long bones from the Sima de los Huesos (SH) Middle Pleistocene site, in the Sierra de Atapuerca, makes it possible to calculate for the first time the absolute bone volume in five complete long bones (two femora and three humeri) of a fossil human species, an approach not possible in fragmentary or poorly preserved fossils. We have relied on computed tomography scans and 3D reconstructions to calculate bone volume. A sample of 62 complete bones of robust recent humans was also used for comparative purposes. The male SH femora (weight-bearing bones) and humeri (non-weight-bearing bones) have, relative to their size, greater bone volume (volume of bone tissue over total bone volume) than the equivalent bones in our recent human sample. As mass is volume $\times$ density, and bone tissue density (as a material) is similar across mammals, we calculate bone mass, and our results show that the SH hominins had on average heavier long bones than extant humans of the same size. From the femoral weight at hand, we have estimated the total skeletal weight in two SH individuals, which is about 36% heavier than in the recent humans of the equivalent body size. Using different methods and skeletal variables, including skeletal weight, to estimate body mass in these two SH humans, we highlight the considerable differences in body mass estimates we obtained, and that the largest body mass estimate is the one based on the skeletal weight. Our results suggest that we cannot assume the same relative proportion of bone volume and bone and skeletal weight characterized the entire genus *Homo*. Given that skeletal weight has a significant influence on body mass, current body mass estimates of fossil *Homo* specimens could be systematically underestimated. Thus, the significantly larger bone volume and heavier bones, probably throughout the entire skeleton, of SH humans could have had consequences for many biological parameters in this Pleistocene population and considerable importance for studies focusing on adaptive and ecologically relevant characteristics. Although more recent human samples should be analyzed, in our view, the high skeletal robusticity of the SH sample, including larger bone volume and skeletal weight, is part of their adaptive body type selected for throughout the Pleistocene to support different mechanical and activity regimes and formed under tight genetic control, including control over bone formative and regulatory processes.

Key words: body mass; bone quantity; CT-scan; hominins; long bones.

Correspondence
José-Miguel Carretero, Dpto. de Historia, Geografía y Comunicación, Laboratorio de Evolución Humana, Universidad de Burgos, Edificio I+D+i, Plaza Misael Bañuelos s/n, 09001 Burgos, Spain. T: +34 947 25 93 24; E: jmcarre@ubu.es

Accepted for publication *20 August 2018*
Article published online *2 October 2018*

Introduction and objectives

A generally elevated level of skeletal 'robusticity' has been extensively documented among Pleistocene non-*Homo sapiens* (archaic) humans, and numerous studies have analyzed the cortical area and cross-sectional parameters

in fossil long bones, pointing out important differences from living humans (for review, see Trinkaus & Ruff, 2012). Despite extensive information on long bone cross-sectional properties at different diaphyseal levels, as part of this pattern of skeletal robusticity, the total bone volume of a fossil human (and hominin) bone has never been calculated in any specimen, mainly due to their generally fragmentary nature. The large sample of Middle Pleistocene human fossils from the Sima de los Huesos (SH; circa 430.000 years BP; Arsuaga et al. 2014) is a rare exception and includes 27 complete long bones, several of them in an exceptional external and internal state of preservation. This provides an opportunity to directly calculate the true bone volume in fossil hominin limb long bones and compare this with recent humans.

Researchers have long appreciated the significant relationship between body size and an organism's adaptive strategy and life history (Damuth & MacFadden, 1990), and body mass estimation in fossil human species is a crucial topic in paleoanthropology (Ruff & Niskanen, 2018) as it yields information about ecologically relevant characteristics. Skeletal weight is a significant portion of the body mass and comprises, on average, approximately 14% of the body mass in modern humans (Shephard, 1991; Clarys et al. 1999; Zilhman & Bolter, 2015). Therefore, changes in skeletal weight during our evolutionary history would have affected numerous adaptive and ecologically relevant characteristics, such as biomechanical efficiency (Ruff et al. 1991), energetic requirements (Froehle & Churchill, 2009), skeletal growth and development (Ruff, 2003), pregnancy and childbirth (Aiello & Key, 2002), brain growth (Ponce de Leon et al. 2008), encephalization (Ruff et al. 1997) and population growth (Sorensen & Leonard, 2001), among others.

The increased postcranial diaphyseal robusticity in archaic members of the genus *Homo* has been argued to be a developmental response to increased mechanical loading of the skeleton applied during the lifetime rather than being genetically determined (Ruff et al. 1993, 1994; Trinkaus et al. 1994; Holt, 2003; Shackelford, 2007). Nevertheless, current evidence also suggests that genetic factors contribute significantly to the regulation of bone mass and that it is a highly heritable trait (Churchill, 1996, 1998; Lieberman, 1996; Pearson & Lieberman, 2004; Ruff et al. 2006), so the debate is not settled.

Therefore, exploring bone volume is worthy of study because it is directly related to skeletal robusticity, which has been considered to be the most important variable for determining bone weight. Bone weight, in turn, is a relevant variable to estimate skeletal weight (Ingalls, 1931; Trotter, 1954; Baker & Newman, 1957), a parameter that is directly related with body mass. Estimates of bone volume and skeletal weight in fossil hominins then could provide new insights into several aspects of their anatomy and physiology compared with recent humans.

The purpose of the present study was to: (i) directly calculate bone volume in the best preserved femora and humeri of the Middle Pleistocene humans from the SH sample; (ii) calculate bone weight from bone volume, relying on the known density of bone across mammals (see below); (iii) estimate skeletal weigh in several individuals from the SH; and (iv) compare these parameters with recent *H. sapiens* samples. The implications of our results (differences in these parameters between species) and hypotheses about the origin of the skeletal robusticity in archaic humans, including those from the SH, can be explored.

Materials and methods

Fossil and comparative samples

The SH site in the Sierra de Atapuerca (Burgos, Spain) contains an accumulation of Middle Pleistocene human fossils that are widely considered to be ancestral to the Neandertals and represent their sister group (Arsuaga et al. 2014, 2015). To date, the SH site has yielded nearly 7000 human fossils representing at least 28 individuals. The human fossils from the SH site have been dated to about 430 Ka (Arsuaga et al. 2014).

To calculate bone volume, we have relied on the most complete adult long bones in the sample that preserve intact outer surfaces and inner structures. Five bones fulfill these preservation conditions: femora X (left) and XIII (right); and humeri II (right), X (right) and XV (left; Fig. 1). These five long bones have been sexed as adult males (Carretero et al. 2012).

For comparative purposes, we analyzed 42 complete adult modern human femora (23 females and 19 males) from a Medieval cemetery at San Pablo Monastery in Burgos (Spain), and 17 adult male femora and 20 adult male humeri from a contemporary forensic collection of known sex housed at the Laboratorio de Evolución Humana (LEH) at the University of Burgos. We have pooled

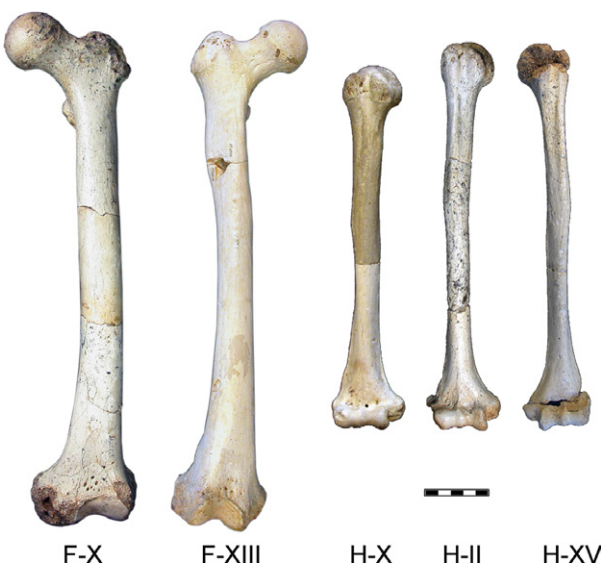

Fig. 1 Virtually complete femora and humeri from the Sima de los Huesos (SH) site analyzed in this study.

together all specimens in a single sample we call LEH Recent Humans, composed thus of 59 femora (36 males and 23 females) and 20 male humeri (Table 1).

The sex of the Medieval San Pablo skeletons was assessed based on the associated pelvic remains. Modern human forensic anatomical collections are often composed of elderly or geriatric individuals, and bone mass is known to decrease with increasing adult age in males and females. We have attempted to control for this factor by only including skeletons of individuals with an estimated age at death of less than 50 years and with no apparent skeletal signs of pathological conditions. The age at death of individuals in these comparative samples has been estimated based on established criteria for the pubic symphysis, iliac auricular surface and the sternal end of the ribs (White & Folkens, 2000). The mean age at death of the entire Medieval sample is 33.7 years with a range between 19 and 49 years.

Our Medieval sample likely consists of individuals who lived in a rural setting and whose lifestyles involved manual labor, while the contemporary sample consists of pre-civil war Spaniards. None of these individuals represents Hunter–Gatherer populations, which in terms of physical activity levels and robusticity would be the most appropriate comparison with the fossil hominins (Ruff et al. 1993, 1994; Trinkaus et al. 1994; Holt, 2003; Auerbach & Ruff, 2004; Shackelford, 2007; Rodríguez et al. 2018). However, to ensure the suitability of these samples for comparison with the fossil specimens, we calculated the % cortical area (%CA) at the femoral midshaft (a parameter that expresses robusticity) and compared this with other Holocene and Pleistocene samples. In both the cortical thickness at midshaft and bone density, our recent human samples are well within the range of Neolithic and Amerindian Hunter–Gatherer samples, making them suitable for comparisons with the fossils (Fig. 2). Given the similar levels of robusticity in both our two recent samples (San Pablo Medieval and Contemporary Spaniards), we combined all specimens into a single pooled sample (LEH Recent Humans). Because data in the literature for bone volume in archaeological or osteological collections are very scarce (indeed, nearly non-existant), we have included the data for our female sub-sample as this may be useful for future research. Nevertheless, only the recent male sub-sample was used for comparisons with the SH specimens that were sexed as males.

Computed tomography scanning and virtual reconstructions

Computed tomography (CT) images of the fossil and recent specimens were captured with a YXLON Compact (YXLON International X-Ray GmbH, Hamburg, Germany) industrial multi-slice CT scanner, housed at the Universidad de Burgos. Specimens were aligned along the long axis of the bone. Scanning parameters included scanner energy of 160 kV and 4 mA. The field of view is variable due to the different size of bones in the sample, and ranges between 90 and 170.3 mm. Slices were obtained as a 1024 × 1024 matrix of 32-bit float format for processing with an interslice distance of 0.5 mm. The pixel size ranges throughout the complete

Table 1 Absolute and RBV (in cm^3)* in the SH fossils and recent human samples.

Sample	SEX	*N*	TEV	*Z*-score† TEV SH and RHs males	SBV	*Z*-score SBV SH and RHs males	RBV‡	*Z*-score RVB SH and RHs males	Difference§ in RBV between SH and RHs males
Femur									
SH Femur X (L)	M	1	637.7	2.1	400.1	5.3	62.7%	2.5	17.6%
SH Femur XIII (R)	M	1	501.5	0.4	318.7	3.0	63.6%	2.7	18.5%
SH Mean	M	2	569.6	1.2	359.4	4.1	63.1%	2.6	18.0%
LEH Recent	M	36	471.7 ± 78.7		210.6 ± 36.1		45.1 ± 6.8%		
Homo sapiens			(316.4–613.0)		(118.7–271.2)		(30.9–59.3)		
(this study)	F	23	328.7 ± 39.2		146.7 ± 29.8		44.6 ± 6.7%		
			(261.0–415.8)		(88.4–207.2)		(31.8–58.9)		
	M+F	59	415.9 ± 96.2		185.7 ± 45.9		44.9 ± 6.7%		
Humerus									
SH Humerus II (R)	M	1	181.3	1.0	138.0	3.5	76.1%	4.2	17.2%
SH Humerus X (R)	M	1	171.9	0.6	118.6	2.0	69.0%	2.4	10.1%
SH Humerus XV (L)	M	1	135.9	−1.0	100.2	0.6	73.7%	3.6	14.8%
SH Mean	M	3	163.1 ± 24.0	0.2	119.0 ± 18.9	2.0	73.0%	3.4	14.1%
LEH Recent	M	20	158.3 ± 23.6		92.8 ± 12.8		58.9 ± 4.1%		
Homo sapiens			(110.1–197.6)		(65.3–112.7)		(51.0–68.0)		
(this study)									

*Values in cm^3 and adjusted to one decimal place to make reading easier (i.e. mm^3 divided by 1000).

†The *Z*-score is the normalized difference between the recent human sample mean and the observed value of the fossil specimens, i.e. the number of standard deviations a datum is above/below the mean. It is calculated as the datum minus the reference mean divided into the standard deviation of the reference sample. In this way, we have calculated a different *Z*-score for each variable and relative to each comparative sample, considering values below or above 1.96 SD statistically significant (Sokal & Rohlf, 1979).

‡RBV = 100 × (SBV/TEV).

§Absolute difference between SH value and LEH recent human male sample mean.

LEH, Laboratorio de Evolución Humana; RBV, relative bone volume; RHs, Recent Homo sapiens; SBV, structural bone volume; SH, Sima de los Huesos; TEV, total enclosed volume.

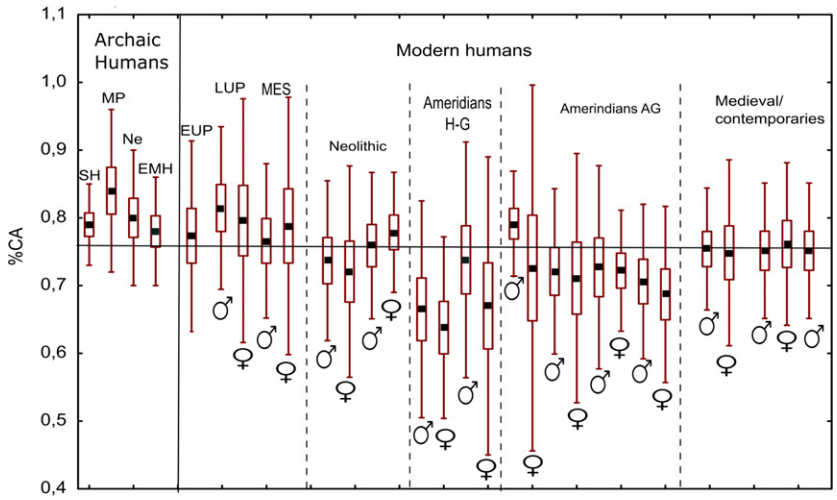

Fig. 2 Comparison of percentage cortical area (%CA) at the femoral midshaft cross-section in several fossil and recent human samples. SH = Sima de los Huesos ($N = 5$; Rodríguez et al. 2018); MP = other Middle Pleistocene specimens ($N = 17$; Trinkaus & Ruff, 2012); Ne = *Homo neanderthalensis* ($N = 18$; Trinkaus & Ruff, 2012); EMH = Early Modern Humans ($N = 10$; Trinkaus & Ruff, 2012); EUP = Early Upper Paleolithic ($N = 38$; Trinkaus & Ruff, 2012); LUP = Late Upper Paleolithic ($N = 17$, 12 males, five females; Trinkaus & Ruff, 2012); MES = Mesolithic ($N = 31$, 23 males, eight females; Marchi, 2008); Neolithic ($N = 58$, 34 males, 24 females; Marchi, 2008; Sparacello & Marchi, 2008); Amerindians H–G = Hunter–Gatherers ($N = 44$, 20 males, 24 females; Larsen et al. 1995) Amerindians AG = Agriculturalist ($N = 222$, 117 males, 105 females; Larsen et al., 1995); Medieval/Contemporaries – from left to right: males and females from Sparacello & Marchi (2008; $N = 77$); males ($N = 36$) and females ($N = 23$) from San Pablo this study; and Contemporary Spanish males ($N = 20$) this study.

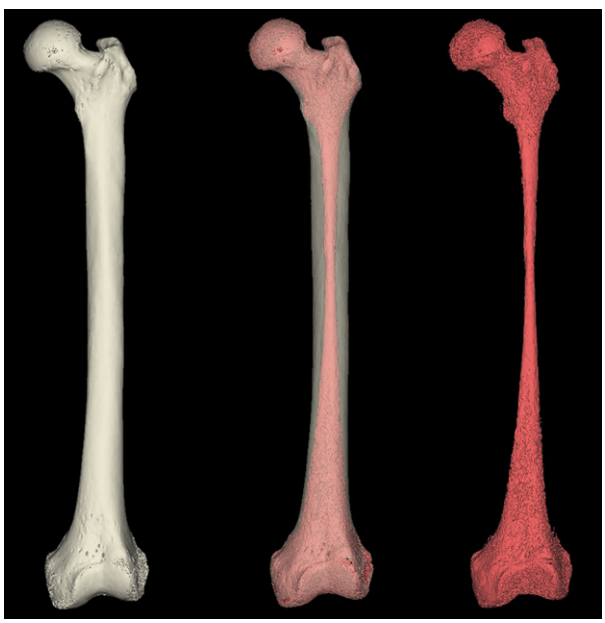

Fig. 3 seBone segmentation to separate air from bone in contemporary Femur 56 from the Laboratorio de Evolución Humana (LEH) collection using the MIMICS software program and semiautomatic segmentation (see text for details). Air contained within the bone is shown here in red.

sample from 0.08 mm for the smaller humeri to 0.181 mm for the bigger femora (pixel size varies with image size). Scans were collected at the maximum resolution obtainable and used to obtain 3D reconstructions of the long bones. The MIMICS software program (Materialise, Belgium) was used to calculate bone volumes using semiautomatic segmentation in order to define and distinguish Hounsfield values for bone (with an emphasis on distinguishing trabecular bone) and air (Figs 3 and 4).

Nevertheless, taking measurements from CT scans involves the complication that the imaged structures have inevitably blurred boundaries. At the boundary of a structure, or at any tissue interface, the CT numbers change from the level of one tissue to that of another, but this change is gradual rather than abrupt owing to the limited spatial resolution (e.g. bone–air interface or dense cortical bone–light trabecular bone interface). The CT number is the value [in Hounsfield units (HU)] assigned to each pixel expressing the local X-ray attenuation in the slice of the scanned object and, in a CT image, these numbers are selectively translated into the gray levels shown on the computer screen. In studies based on phantoms as well as extant and fossil bone, it has been shown that the interface is located exactly halfway between the two CT number levels on either side of the structure boundary (Spoor et al. 1993). This level, known as half-maximum height, equals the mean of the two CT number levels at either side of the interface.

In the present study, it is important not to add cortical bone tissue at the outer surface of the bone, as this would increase the bone volume. At the same time, we also want to retain the trabecular bone (even though this contributes only a small percentage of the total long bone mass), which is much less dense (lower CT numbers) than cortical bone (higher CT numbers). If we use the half-maximum height CT number between cortical bone and air, much of the trabecular bone will not be included. Conversely, using the half-maximum height, CT number between trabecular bone and air would be adding considerable cortical bone at the outer surface. Given these complications, we have followed a 'semi-automatic' protocol to define the limit between air and bone.

In addition to the gray-scale, MIMICS software provides three pseudo-color scales that aid in viewing the image data. The pseudo-color scales vary the hue (color) and luminance (brightness) within the images. Using color scales, small differences in the soft tissue or

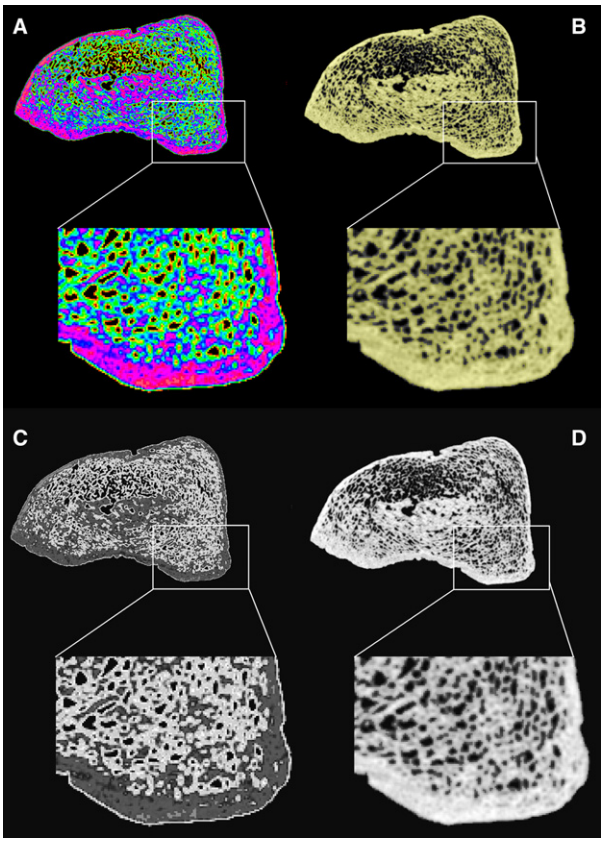

Fig. 4 Details of the semiautomatic segmentation in a cross-section of the distal epiphysis for Femur X showing the differences in bone/air quantities before and after the process. Above full spectrum color scale to determine Hounsfield Units (HU) for bone and air. (A) Full spectrum image in which all Hounsfield density values are grouped and colored in eight categories. Note that very few pixels are colored as standard air (black). To avoid the border effect and taking into account the computed tomography (CT) numbers, the black, orange, yellow and green pixels have been considered as air (CT number < 176 HU), and the blue, pink, red and white pixels have been considered as bone (CT number > 176 HU). This CT number is very close to 200 HU, the standard value used in medical analysis to separate bone and air (Ciarelli et al. 1991; Oliveira et al. 2008). (B) Bone spectrum image showing the pixels (in HU) considered as bone once those considered as air in the full spectrum image have been eliminated. Air now is in black, and notice the difference in its quantity with full spectrum image. Below the colors have been transformed in a gray-scale. (C) Full spectrum image where very few pixels are colored as standard air (black). Taking into account the CT numbers, here the black and dark gray pixels have been considered as air (CT number < 176 HU), and the white and light gray pixels have been considered as bone (CT number > 176 HU). (D) Bone spectrum image showing the pixels (in HU) considered as bone once those considered as air in the full spectrum image have been eliminated. Air is in black, and notice the difference in its quantity with full spectrum image.

the bone can be enhanced. Unlike the gray-scale, the pseudo-color scales are non-linear. The full spectrum color scale varies within the standard continuous range of hues from orange to yellow to green to blue to pink to red. In order to make air black and bone white, it also varies in luminance from dark (black) to light (white). A scale of eight colors is used automatically by the software (Fig. 4). To ensure we do not artificially add bone volume, we manually established a bone–air limit based on the standard HU fixed by medical analysis, in which Hounsfield densities of about 200 HU are considered trabecular bone (Ciarelli et al. 1991; Oliveira et al. 2008). As mentioned above, the SH fossils are not strongly taphonomically altered, so these medical parameters can be reasonably applied. In the automatic full spectrum color images (Fig. 4), black, orange, yellow and green pixels have CT numbers below 176 HU, while blue, pink, red and white pixels have CT numbers above 176 HU. A CT number of 176 is very close to the value of 200 used in medical analysis (Ciarelli et al. 1991; Oliveira et al. 2008). Thus, we have considered all pixels below 176 HU as air, while pixels above 176 HU are considered to represent bone (see Fig. 4 for details and for the gray-scale version). This has the effect of removing some very-low-density trabecular bone rather than adding denser trabecular or cortical bone. We carried out this segmentation approach in all the fossil and comparative specimens.

Calculation of absolute and relative bone volume and bone weight

We should emphasize that we are not discussing 'bone tissue mineral density' in its physiological sense (i.e. relative proportions of the organic and inorganic components and their chemical properties), but only the absolute and relative bone quantity or bone volume. Although the original bone mineral density can be altered by taphonomic processes, for our purposes here we consider that density of bone tissue, as a material defined by physics (weight divided by volume), is 1.8 g cm^{-3} for the class *Mammalia* (Currey, 2002).

Two different volumes were calculated: a total enclosed volume (TEV) under the bone surface that includes the medullary cavity and air (i.e. total subperiosteal bone volume + air volume); and the structural (i.e. true) bone volume (SBV) that is limited to the cortical and trabecular bone, excluding the air (SBV = TEV – air volume) (Table 1). The TEV has been used as a control variable for bone size instead of any linear articular dimension in the calculation of the relative bone volume (RBV = 100 × SBV/TEV). After the SBV is determined, bone weight can be directly calculated using the bone tissue density mentioned above, and by definition mass is volume × density.

Following this reasoning, we have calculated the absolute bone weight for femora and humeri in both the SH hominins and our recent *H. sapiens* specimens. Nevertheless, it is more interesting to compare bone weight relative to body size between fossil and recent samples. To address this issue, a reduced major axis (RMA) regression line between bone weight and a control variable for body size was derived from our recent male samples of femora (N = 36) and humeri (N = 20), and subsequently applied to the fossil specimens. RMA-type regression analysis better summarizes the relationship between two variables than do alternative regression models (major axis and ordinary least squares) when the aim is not to generate a predictive model or when outliers are expected. Moreover, RMA is the line-fitting technique commonly used in allometry contexts in which the purpose of the study was to describe how size variables are related, typically as a linear relationship on logarithmic scales (Aiello, 1992; Warton et al. 2006). The regression line and its 95% confidence interval were calculated.

As a control variable for body size in our regression analysis, we use femoral and humeral head volume. It is well established that

articular dimensions are proportional to body mass and correlate much better with body size than any other bone dimension, and they are widely used as a proxy for body mass estimation in many paleoanthropological studies (Jungers, 1988; McHenry, 1992; Grine et al. 1995; Ruff et al. 1997, 2005; Auerbach & Ruff, 2004; Arsuaga et al. 2015; Rodríguez et al. 2018; Ruff & Niskanen, 2018). However, because we are comparing volumetric variables and volume increases are proportional to the cube of length (i.e. L^3), we have used a measure of articular size that is expressed in cm^3. The femoral head represents virtually a complete sphere whose volume can be easily calculated ($4/3 \cdot \pi \cdot r^3$; where r is half of the head diameter), and we have relied on this dimension (femoral head volume) as a control variable for body size in the femoral comparisons. In contrast, the humeral head is not spherical, as the vertical and transverse diameter are not even. Humeral head shape is more similar to half of an ellipsoid. Thus, we have calculated the humeral head volume as if it was a complete ellipsoid ($4/3 \cdot \pi \cdot a \cdot b \cdot c$), and the resulting volume was then divided in half. Here, a, b, c are the principal axes of the ellipsoid and can be easily obtained directly, or via 3D bone reconstructions, by measuring the transverse and vertical humeral head diameters and the curvature radius of the humeral head, respectively (Fig. 5; Table 2).

To express the differences in bone weight relative to body size between the fossils and recent samples, we determined the percentage difference between the calculated (observed) values for the fossils and their expected value according to the RMA regression line. We calculated the difference with the mean and with the limits of its 95% confidence intervals (Table 3).

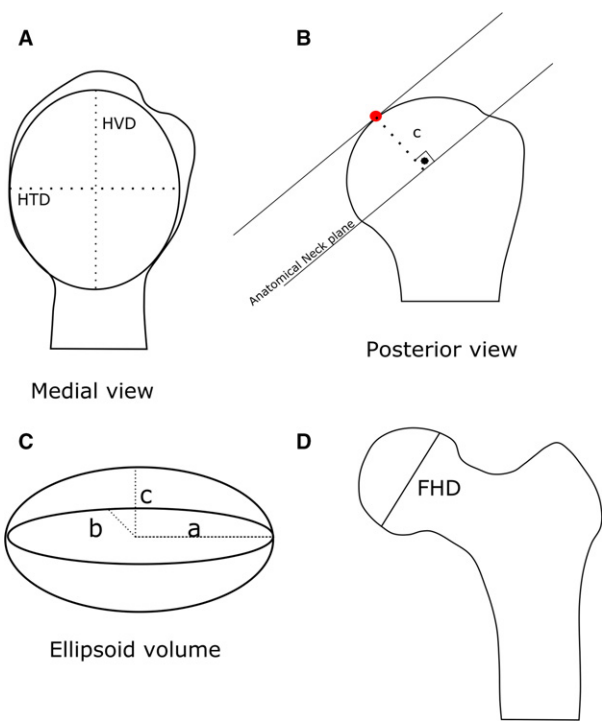

Fig. 5 (A, B) Linear measurements of humeral head used to compute its volume as if it was an ellipsoid (C). HVD, humeral head vertical diameter; HTD, humeral head transverse diameter; C, humeral head curvature radius; D, femoral head diameter.

Calculation of skeletal weight, body mass and daily energy expenditure

Surprisingly, only two studies have been published examining the relationship between femoral weight and skeletal weight since the mid-20th century (Trotter, 1954; Baker & Newman, 1957). Other studies report skeletal weight in Asian, American and European samples (Merz et al. 1956; Lowrance & Latimer, 1957; Silva et al. 2008), but do not specifically relate skeletal weight with femoral weight. According to Trotter (1954) and Baker & Newman (1957), there is a strong relationship ($r = 0.89$–0.96) between dry femoral weight and skeletal weight.

Baker & Newman (1957) provide a regression equation for estimating skeletal weight from femoral weight based on a sample of 95 white male individuals. Trotter (1954) provides the raw data on bone mass and skeletal mass on a sample of 24 individuals of European ancestry, but no regression equation. Thus, we have derived a second regression equation based on her data. This approach yields two different regression equations based on two different recent samples. Because the results derived with one or the other formulae are not significantly different, we averaged the two estimations for all specimens (Table 4).

Relying on this relationship between dry femoral weight and skeletal weight in recent humans, and assuming the same relationship in Pleistocene humans, we have explored the total skeletal weight of two SH male individuals represented by Femur X and Femur XIII compared with recent humans (Tables 4 and 5). To compare skeletal weight relative to body size, we follow the same regression approach described above for bone weight comparisons. In this case, the 'observed' skeletal weight is the average of the two formulae mentioned above and, with these data, we derived a RMA regression line of skeletal weight on femoral head volume from our recent male sample ($N = 36$). This RMA regression line was applied to the two SH specimens, and the percentage differences between observed and expected values were calculated (Table 5).

Finally, to investigate the possible consequences of larger bone volume and skeletal weight in the SH humans, we have estimated two important biological parameters in these fossil humans: body mass and daily energy expenditure (Table 6). Among the SH sample we have associated Femur X with the complete Pelvis 1 (Arsuaga et al. 1999; Bonmati et al. 2010) and, elsewhere, we have determined a stature of 170 cm for this individual, and 167.8 cm for Femur XIII (Carretero et al. 2012). Using different regression equations that relate femoral head dimensions and stature-bi-iliac breadth relationship to body mass in recent humans (Grine et al. 1995; Ruff et al. 1997, 2005; Auerbach & Ruff, 2004), the body mass of individuals represented by isolated Femur XIII and Femur X on the one hand, and Femur X plus Pelvis 1 on the other, can be determined (Arsuaga et al. 2015). These estimations are compared with those derived from bone and skeletal weight calculated in the present study (Table 6).

On the other hand, previous studies have suggested higher energy requirements (about 100–350 kcal day^{-1}) in Neandertals as compared with modern humans in similar climates, and this difference is in large part due to greater body mass in Neandertals (Froehle & Churchill, 2009). Following these authors (see Table 6 for methodological details on daily energy expenditure calculations), the daily energy expenditure was estimated for two SH males represented by Femurs X and XIII based on the minimum and maximum body mass estimates (Table 6).

Table 2 Femoral and humeral head raw parameters (in mm) used to calculate their respective head volumes (in cm^3).

Sample	Femoral head diameter*	Humeral head transverse diameter*	Humeral head vertical diameter*	Humeral head curvature radius*	Head volume†
Femora					
SH Femur X	52.5				170.5
SH Femur XIII	48.3				132.8
LEH recent males ($N = 36$)	47.3 ± 2.8 (42.3–54.9)				56.1 ± 10.4 (39.6–87.0)
LEH recent females ($N = 23$)	43.1 ± 2.8 (38.2–50.9)				41.3 ± 6.9 (29.1–62.7)
LEH recent (M + F) ($N = 59$)	45.8 ± 3.4				50.9 ± 11.7
Humeri					
SH Humerus II		46	44.2	20.3	44.9
SH Humerus X		48	44.4	20.43	45.6
SH Humerus XV		44	42	17.69	34.2
LEH recent males ($N = 20$)		43.7 ± 2.63 (38.9-48.5)	42.9 ± 4.47 (36.4–50.5)	20.3 ± 1.68 (17.2–23.6)	20.2 ± 4.3 (14.8–28.4)

*See Fig. 5 for variable definitions.
†Femoral head volume was calculated as if it was a complete sphere: $4/3 \cdot \pi \cdot r^3$. Humeral head volume was calculated as if it was a half-ellipsoid: $4/3 \cdot \pi \cdot a \cdot b \cdot c$, and then half divided. a, b and c are the principal axes of the ellipsoid: a = humeral head vertical diameter/2; b = humeral head transverse diameter/2; c = humeral head radius (maximum orthogonal distance from the anatomical neck to the humeral head articular surface; can be also measured on the CT image).
LEH, Laboratorio de Evolución Humana; SH, Sima de los Huesos.

Table 3 Bone weight comparisons between the SH fossils and our recent *Homo sapiens* sample.

Sample	Sex	*N*	Calculated bone weight (g)*	Expected bone weight (g)†	Percentage difference‡
Femur					
SH Femur-X	M	1	720.1	520.7 (500.4–529.3)	38.3% (36.1–43.9%)
SH Femur- XIII	M	1	573.7	402.3 (410.9–381.9)	42.6% (39.6–50.2%)
SH Mean		2	646.9	461.5	40.4%
LEH Recent	M	36	379.1 ± 64.9 (213.7–488.2)		
H. sapiens (this study)	F	23	264.1 ± 53.7 (159.1–373.0)		
	M+F	59	334.3 ± 82.7		
Humerus					
SH Humerus II	M	1	248.4	179.25 (170.7–189.7)	38.6% (30.9–45.5%)
SH Humerus X	M	1	213.5	181.0 (172.5–191.5)	17.9% (11.5–23.8%)
SH Humerus XV	M	1	180.4	150.8 (142.3–161.3)	19.6% (11.9–26.8%)
SH Mean		3	214.1 ± 34.0	170.3	25.4%
LEH Recent *Homo sapiens* (this study)	M	20	167.0 ± 23.0 (117.6–202.8)		

*Calculation of bone weight relies on the SBV (Table 1) and a bone density of 1.8 g cm^{-3}, the density value in class *Mammalia* (Currey, 2002). By definition: mass = volume × density.
†Predicted bone weight (mean and its 95% confidence interval limits) by the RMA regression lines of bone weights on head volumes derived from our LEH recent human sample. HW = 59.63 + 5.33 × HHV ± 19.1 (SE); $N = 20$; $R = 0.59$, $p < 0.01$. (HW = humerus weight; HHV = humeral head volume). FW = −14.47 + 7.06 × FHV ± 66.0; $N = 36$; $R = 0.61$, $P < 0.01$. (FW = femur weight; FHV = femoral head volume). See Figs 5 and 6 for more details.
‡Percentage difference between calculated and expected bone weights (mean and its 95% confidence interval limits) for SH fossils specimens. Percentage difference = 100 x (calculated value – expected value)/(expected value).
LEH, Laboratorio de Evolución Humana; SH, Sima de los Huesos.

Table 4 Comparisons of skeletal weights (g) in several recent human samples and from different sources.

Sample	Baker and Newman formulae*	This study formulae†	Mean of the two previous formulae‡	Other sources
LEH Recent *Homo sapiens* males, $N = 36$ (this study)	4021.9 ± 573.9 (2559.9–4986.8)	4290.5 ± 591.0 (2785.1–5284.0)	4217.6 ± 517.2 (2699.5–5132.1)	
LEH Recent *Homo sapiens* females, $N = 23$ (this study)	3005.5 ± 474.8 (2076.5–3968.2)	3243.9 ± 488.8 (2287.4–4235.1)	3122.3 ± 420.2 (2202.1–4072.8)	
LEH Recent *Homo sapiens* M + F, $N = 59$ (this study)	3625.7 ± 730.9	3882.5 ± 752.6	3804.3 ± 718.7 (2202.1–5132.1)	
American male from Terry Collection, $N = 24$	4181 ± 762 (2615–5842)	4454 ± 785 (2842–6165)	4318 ± 774 (2729–6003)	4459.9 ± 800.8§ (3075–6128)
Male American whites¶, $N = 100$				4956.9 ± 719.8 (2984–6976)
Coimbra males**, $N = 50$				3850.0
Coimbra females**, $N = 50$				2797.6
Coimbra M + F**, $N = 100$				3323.8 ± 779.6
Asiatic sample M + F††, $N = 105$				2882.0 ± 365.0
White male Terry Collection‡‡, $N = 55$				4417.0 ± 645.8
Black male Terry Collection‡‡, $N = 54$				5068.9 ± 821.9

*Least-squares regression formulae: SKW = 8.84 (FW) + 670.24 ± 278 g (SE); $N = 95$; $r = 0.89$ (Baker & Newman, 1957).
†Least-squares regression formulae: SKW = 9.10 (FW) + 839.41 ± 237 g (SE); $N = 24$; $r = 0.96$ (derived by the authors with the raw data in Trotter, 1954).
FW, femur weight; SKW, skeletal weight.
‡Average of estimates with the formulae in * and †.
§Actual mean and SD of the sample reported by Trotter (1954).
¶From Ingalls (1931).
**From Silva et al. (2008).
††From Lowrance & Latimer (1957).
‡‡From Merz et al. (1956).
LEH, Laboratorio de Evolución Humana.

Table 5 Comparison of two different estimates of skeletal weight (g) derived from SH femora.

	Skeletal weight derived from femur weight*	Skeletal weight derived from femoral head volume†	Percentage difference between both estimates
	Estimate A	Estimate B	100 × (A – B)/(B)
SH Femur-X	7215.8	5337.8 (5112.6–5512.8)	35.2% (30.9–41.1%)
SH Femur-XIII	5902.0	4329.1 (4014.7–4414.9)	36.3% (33.7–47.0%)

*Average of estimated skeletal weight (SKW) from femur weight (FW) calculated with two least-squares regression formulae in Table 4: SKW = 8.84 (FW) + 670.24 ± 278 g (SE); $N = 95$; $r = 0.89$ (Baker & Newman, 1957). SKW = 9.10 (FW) + 839.41 ± 237 g (SE); $N = 24$; $r = 0.96$ (derived by the authors with the raw data in Trotter, 1954).
†Estimated skeletal weight (SKW) from femoral head volume (FHV) calculated with a RMA regression line derived from our LEH recent human male sample (mean and 95% confidence intervals limits): SKW = 780.3 + 60.15 × (FHV) ± 515.8 g (SE); $N = 36$; $r = 0.68$; $P < 0.01$. Individual skeletal weights of the 36 recent specimens used in the RMA regression line construction, calculated as the mean of the two formulae in footnote*.
SH, Sima de los Huesos.

Results

Absolute and relative SBV

In absolute values (Table 1), the TEV of the SH femora and humeri is not especially large compared with our recent human samples. Although Femur X falls above the range of variation in recent human males, Femur XIII and all three SH humeri fall within ± 1 standard deviation (SD) of the corresponding recent male means (Table 1). However, the absolute structural (true) bone volume in both SH femora falls well above the range of variation in recent males (5.3 and 3 SD above the male recent mean, respectively; Table 1). Among the humeri, only Humerus XV (left side) is close to the recent sample mean, while Humeri X and II fall above the upper limit of the range of variation (Table 1).

The RBV, calculated as the proportion of SBV to total bone volume, is very similar in both SH femora, despite

Table 6 Comparisons of body mass (kg) relying on different regression formulae, and two energetic parameters (kcal per day) in two SH males and two human fossil samples.

Raw variables used to estimate body mass (BM)	FHD (cm)	SK-BIB (cm)	L-BIB (cm)	ST* (cm)
Male Femur X + Pelvis 1	5.25	34.0	36.8	170.0
Femur XIII	4.83			167.8

	Body mass formulae					
	FHD[†]	FHD[‡]	ST-BIB[§]	ST-BIB[¶]	SKW**	FW[(f)]
Male Femur X + Pelvis 1						
Body mass (BM)	80.1	82.1	92.5	93.8	99.4	102
Basal metabolic rate (BMR)[††]	1847	1884	2029	2048	2131	2169
Daily energy expenditure (DEE)[‡‡]	3565	3636	3917	3954	4112	4186
DEE difference with Neandertal mean (see below)	126	197	478	515	673	747
DEE difference with EAMH mean (see below)	402	473	754	791	949	1023
Male Femur XIII						
BM	69.7	73.3			86.8	88.2
BMR (kcal per day)	1694	1743			1946	1966
DEE (kcal per day)	3270	3365			3755	3795
DEE difference with Neandertal mean (see below)	−169	−74			316	356
DEE difference with EAMH mean (see below)	107	202			592	632
Male Neandertals of temperate climate[§§]						
Mean BM			75.8			
BMR (mean, SD and range)			1782 ± 62 (1672–1851)			
DEE (mean, SD and range)			3439 ± 118 (3227–3572)			
Male EAMH of temperate climate[¶¶]						
Mean BM			66.0			
BMR (mean, SD and range)			1639 ± 165 (1397–1922)			
DEE (mean, SD and range)			3163 ± 318 (2692–3710)			

FHD, femoral head diameter; SK-BIB, skeletal bi-iliac breadth; L-BIB, living bi-iliac breadth = 1.17 × SK-BIB – 3.0; (Ruff et al. 1997); ST, stature; ST-BIB, stature bi-iliac breadth relationship; SKW, skeletal weight; FW, femoral weight; BMR, basal metabolic rate in kcal per day; DEE, daily energy expenditure in kcal per day; EAMH, early anatomically modern humans.

*Stature in cm from Carretero et al. (2012).

[†]Based on FHD BM estimation equations in Auerbach & Ruff (2004). Formula for males: BM = (2.741 × FHD – 54.9) × 0.90; $r = 0.50$.

[‡]Based on FHD BM estimation equation in Grine et al. (1995). Formula for pooled sex sample: BM = 2.268 × FHD – 36.5.

[§]Based on stature/bi-iliac breadth regression formula in Ruff et al. (1997). Formula for males: BM (kg) = 0.373 × ST (cm) + 3.033 × L-BIB (cm) – 82.5; $r = 0.90$.

[¶]Based on stature/bi-iliac breadth regression formula in Ruff et al. (2005). Formula for males: BM (kg) = 0.422 × ST (cm) + 3.126 × L-BIB (cm) – 92.9; $r = 0.913$.

**Based on regression formulae derived from skeletal weight and femur weight in Baker & Newman (1957).

[††]BMR in kcal per day for each BM in the same column. From Froehle & Churchill (2009). BMR = the energy the body uses for maintenance and growth in the absence of activity or digestion. Most often BMR is estimated from BM. BMR formulae for males = (14.7 × BW) – (5.6 × TMEAN) + 735, where BW is body mass in kg and TMEAN is the mean annual temperature in °C. Mean annual temperature for SH humans = 11.67 °C, calculated by Blain et al. (2009) for the human occupations in TD10 level from Gran Dolina site, also in Sierra de Atapuerca, within the same chronological range of Sima de los Huesos.

[‡‡]DEE in kcal per day for each of BM in the same column. From Froehle & Churchill (2009). DEE = BMR × PAL, where PAL is physical activity level, a coefficient expressing DEE as a multiple of BMR. In the present study, the PAL used by Froehle & Churchill (2009) for temperate climate male Neandertals with high activity levels is = 1.93.

[§§]Data reported by Froehle & Churchill (2009). BM estimated from stature and bi-iliac breadth for Kebara 2, Kiik-Koba; Krapina 213, Regordou 1, Shanidar 1, Shanidar 2, Shanidar 3, Shanidar 4 and Shanidar 5; $N = 9$.

[¶¶]Data reported by Froehle & Churchill (2009). BM estimated from stature and bi-iliac breadth for Bauosse de Torre 2, Caviglione 1, Crogmanon 1, Crogmanon 3, Grotte des Enfants 4, Kubbaniya, Nazalet and Khater 1, and from stature for Batadomba Lena1 and Liujiang; $N = 10$.

more pronounced differences in the total volume between these two specimens. The RBV in the SH femora is 17.6% (Femur X) and 18.5% (Femur XIII) higher than the recent male mean of our sample (Table 1). In the case of the arm bones, the RBV in the SH humeri is between 10.1% (Humerus X) and 17.2% (Humerus II) higher than the recent

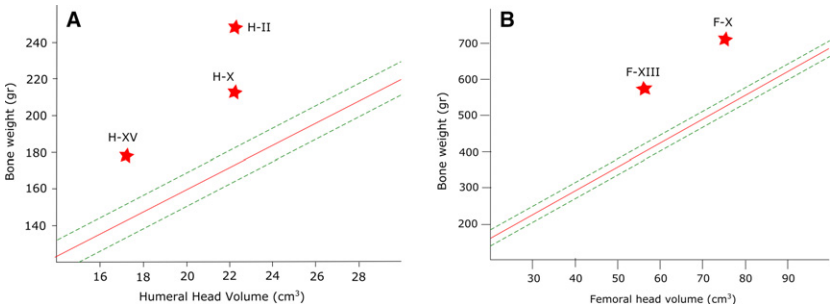

Fig. 6 (A) Reduced major axis (RMA) regression line of humerus weight (HW) on humeral head volume (HHV) and its 95% confidence intervals derived from the Laboratorio de Evolución Humana (LEH) male recent humans sample ($N = 20$). HW = 59.63 + 5.33 × HHV ± 19.1 (SE); $N = 20$; $r = 0.59$, $P < 0.01$ 95% confidence limits = ± 1.96 × SD. (B) RMA regression line of femur weight (FW) on femoral head volume (FHV) and its 95% confidence intervals derived from LEH male recent humans sample ($N = 36$). FW = −14.47 + 7.06 × FHV ± 66.0 (SE); $N = 36$; $r = 0.61$, $P < 0.01$. 95% confidence limits = ± 1.96 × SD.

male mean value (Table 1). Indeed, the values for the RBV in all five SH bones analyzed fall above the modern human range of variation. Although, as mentioned above, the five SH bones analyzed here are sexed as males, it is important to note that the femoral RBV shows no statistical difference between males and females in recent *H. sapiens* (Seeman, 1997), including the sample used in the present study. Moreover, the degree of size variation (interpreted as mainly reflecting sexual dimorphism) in most postcranial dimensions in the SH hominins is similar to that found in recent humans (Lorenzo et al. 1998). Therefore, it is plausible to suggest that our results for the RBV in male SH bones likely characterize female bones from this sample as well.

Within our recent human sample, there is one individual with the same femoral head diameters as Femur X. To the extent that femoral head size is a good expression of body mass (Grine et al. 1995; Ruff et al. 1997, 2005; Auerbach & Ruff, 2004), we can directly compare these two specimens. The TEV (547.5 cm^3), SBV (218.0 cm^3) and RBV (39.8%) of the recent specimen are far removed from the values exhibited by Femur X for the same variables (TEV = 637.7 cm^3; SBV = 400.1 cm^3; RBV = 62.7%; Table 1). A second recent human individual shows the same femoral head diameter and very similar TEV (499.4 cm^3) as Femur XIII (501.5 cm^3), indicating both bones are similar in overall size. However, SBV (251.8 cm^3) and RBV (50.0%) of this recent specimen are again far below the values exhibited by Femur XIII for these same variables (SBV = 318.7 cm^3 and RBV = 63.6%).

Absolute and relative bone weight

Regarding absolute bone weight (volume × density), the dry weights of Femurs X and XIII would have been 720.1 and 573.7 g, respectively, values that fall well above the range of variation in our recent *H. sapiens* samples of comparison (Table 3). The dry weights of the three SH humeri range from 180.4 to 248.4 g, and the mean value for the three SH specimens (214.1 g) again falls above the range of variation in our recent *H. sapiens* samples (Table 3).

As indicated by the regression analysis of bone weight on femoral and humeral head volumes in recent humans (Fig. 6), the SH specimens fall well above the regression line and outside the 95% confidence limits. This clearly indicates that the SH hominins had relatively much heavier femora and humeri than our recent specimens of the same articular size (as a proxy for body size). Expressed as percentage differences, Femur X is 38.3% and Femur XIII 42.6% heavier than their recent counterparts. The SH humeri vary between 17.9% (Humerus X) and 38.6% (Humerus II) heavier than recent humans (Table 3).

Absolute and relative skeletal weight in two SH individuals

The skeletal weights based on femoral weight in both SH male individuals (Femur X = 7215.8 g; Femur XIII = 5902.0 g) fall well above the range of variation in our recent human male samples (Fig. 7A; Tables 4 and 5). Femur X is 5.8 SD and Femur XIII 3.3 SD above our male sample mean (4217.6 ± 517.2 g). The regression analysis of skeletal weight on femoral head volume in recent humans also shows that the skeletal weights in the SH specimens are far above their predicted values for their femoral head volume (Fig. 7B; Table 5). The difference between estimates of skeletal weight based on femur weight and based on femoral head volume is considerable, and estimates are always larger based on femur weight. The percentage difference of the two SH individuals with the recent male mean is very similar (Femur X = 35.2% and Femur XIII = 36.3%; Table 5). These differences clearly indicate that the SH hominins had relatively much heavier skeletons than our recent specimens of the same articular (body) size. The two SH male individuals would have had on average a skeletal weight that was, relative to their body size, nearly 36%

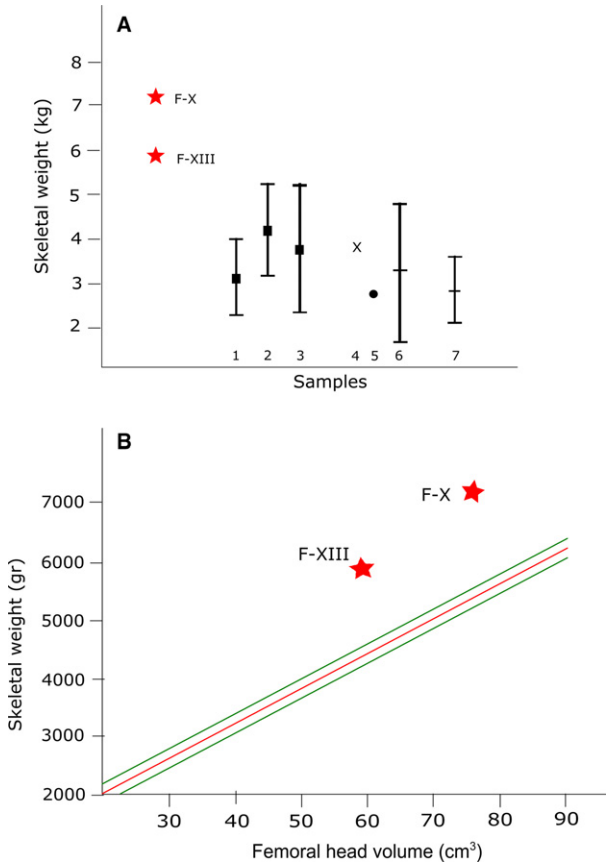

Fig. 7 (A) Absolute estimated skeletal weight in two SH male hominins represented by Femur X and Femur XIII, and several recent *Homo sapiens* samples (mean ± 2 SD). Skeletal weight is the average of estimations calculated with the formulae from Baker & Newman (1957) and the formulae derived by us in this study with the raw data of Trotter (1954). (1) Laboratorio de Evolucíon (LEH) recent females ($N = 23$); (2) LEH recent males ($N = 36$); (3) San Pablo pooled sex sample; (4) Coimbra sample male mean from Silva et al. (2008); (5) Coimbra sample female mean from Silva et al. (2008); (6) Coimbra sample pooled sex mean ± 2 SD from Silva et al. (2008); (7) Asiatic sample mean ± 2 SD from Lowrance & Latimer (1957). (B) Reduced major axis (RMA) regression line of skeletal weight (SKW) on femoral head volume (FHV) and its 95% confidence intervals derived from LEH male recent humans sample: SKW = 780.3 + 60.2 × FHV ± 515.8 (SE); $N = 36$; $r = 0.68$, $P < 0.01$, 95% confidence limits = ± 1.96 × SD.

greater than in the recent human males of our sample (Tables 4 and 5).

Exploring body mass and daily energy expenditure in two SH individuals

Based only on femoral head diameters, the body mass estimated for Femur XIII ranges between about 70 and 73 kg depending on the equation used, and that for Femur X ranges between about 80 and 82 kg. Using the stature-bi-iliac breadth relationship for Femur X + Pelvis 1, we obtain a body mass estimate of about 93–94 kg for this individual. If the skeletons of male SH hominines were approximately 36% heavier than in modern humans as suggested here (Fig. 7; Table 5), the SH individuals may have weighed more than the previous calculations suggest and, in fact, the estimated body masses for these two individuals based on a regression formulae derived separately from both, femoral weight and skeletal weight, range between 87 and 88 kg for Femur XIII and 99 and 102 kg for Femur X (Table 6).

Regarding daily energy expenditure, the estimated value for Femur XIII with the minimum body weight (70 kg) is well below (1.4 SD) the Neandertal male mean, while daily energy expenditure for the maximum body weight (88 kg) is 3 SD above the same mean. For Femur X, the difference in daily energy expenditure from the Neandertal male mean ranges from as low as 126 kcal day^{-1} with the minimum body weight (80 kg) up to 747 kcal day^{-1} with the maximum body weight (102 kg; Table 6). In this case, the first value is only 1 SD above the Neandertal mean, while the second is 6.3 SD above the same mean. The large differences between these estimates highlight the significance of body weight estimates. For example, the difference between the lower and higher estimates of daily energy expenditure for both SH femora are larger in magnitude than the differences we found between the Neandertal and modern human means. Daily energy expenditure differences between SH individuals and Early Modern Humans are very large in any comparison, above all those of Femur X (Table 6).

Discussion and conclusions

The heavy bones and skeletons in the SH adult individuals studied here should have a number of implications. Calcified bone tissue is approximately twice as heavy as other tissues, so it is important for terrestrial species to minimize the weight of the skeleton, even when the skeleton represents a relatively small percentage of the total body weight. Muscle mass is not independent of bone mass (Martin, 2003), and an increase in bone mass results in a proportional increase in muscle mass, as heavier bones require larger, heavier muscles to move them. Because muscle constitutes the largest tissue mass in the human body (Malina & Bouchard, 1991), and the musculoskeletal tissues generally comprise the heaviest organ system in vertebrate animals, increasing skeletal weight clearly influences body mass.

We have estimated the body mass in two SH individuals relying on different methods and skeletal variables, including skeletal weight (estimated from the femoral weight; Table 6). Beyond the specific values obtained for body mass in Table 6, we would highlight both the considerable differences in body mass estimates we obtained using different methods, and that the largest body mass estimate is the one based on the skeletal weight. Thus, could we be in some extent underestimating the body mass in archaic humans?

If heavier skeletons imply heaver bodies, the higher metabolic energy requirements of larger animals should also be considered (Alexander, 1992). Most of the energy required for terrestrial locomotion is not associated with moving the body mass against the force of gravity, but in accelerating and decelerating the oscillating limbs (Hildebrand & Hurley, 1985). Moreover, even small differences in bone mass (e.g. 10%) can be relevant Currey (1984). As the higher predicted energy expenditure values relative to modern humans found in SH males (and the Neandertals) result mainly from larger body size (Table 6), these differences could be even greater than previously thought, as we could be underestimating body mass in these archaic humans without taking into consideration their much heavier skeletons.

Finally, we must also consider that if muscle mass increases in linear proportion to bone mass, as experimental data suggest (Martin, 2003), providing an animal with a lighter skeleton will reduce its body weight and its metabolic energy requirement for locomotion (Alexander, 1992). To make valid comparisons between SH hominines and Early Modern Humans, though, we would want to also take into account the heavier skeletons in the former as that would also factor into their higher activity levels. Although these skeletal differences are still far from being completely demonstrated and evaluated, body mass and energy expenditure are only two examples of the possible consequences derived from significantly heavier skeletons in SH humans relative to recent ones.

Another important question is to determine the origin of these heavier bones and skeletons in the archaic humans. A generally elevated level of skeletal 'robusticity' (bone strength relative to body size) has been extensively documented among Pleistocene non-*H. sapiens* (archaic) humans (Trinkaus & Ruff, 2012), and previous studies have shown that the SH hominins also fit this pattern (Arsuaga et al. 2015; Rodriguez et al. 2016; Rodríguez et al. 2018). The higher RBV (Table 1), higher relative bone weight (Table 3) and higher relative skeletal weight (Table 5) found here are also consistent with these findings.

Although it is well known that skeletal mineralization and bone mass vary with habitual mechanical loads and activity patterns (Rubin & Lanyon, 1984; Forwood & Burr, 1993; Hazelwood et al. 2001; Moisio et al. 2004; Stock, 2006; Maimon & Sultan, 2011), current evidence also suggests that genetic factors contribute significantly to the regulation of bone mass in healthy individuals (McGuigan et al. 2002; Baldock & Eisman, 2004; Judex et al. 2004; Peck & Stout, 2007; Yerges et al. 2010). In fact, it is a highly heritable trait under context-specific genetic regulation whose heritability averages about 60–70% in humans (Ruff et al. 2006).

To what extent is the skeletal robusticity a character strongly linked to the genome (systemic), or whether it reflects mainly the activity of an individual prior to skeletal maturity – the susceptibility of bone to strain is more acute during childhood and adolescence (Ruff et al. 1994; Daly et al. 2004; Pearson & Lieberman, 2004) – is yet to be clearly determined. In this sense, the larger absolute and RBV and bone weight of the SH femora (weight-bearing bones) and humeri (non-weight-bearing bones) partially support the idea of more generalized bone mass differences throughout the skeleton of SH humans. However, we must also consider that in other archaic humans, such as the Neandertals, a higher degree of bilateral asymmetry exists in the upper limb bones, mainly attributable to laterality (i.e. handedness) and activity patterns (Trinkaus et al. 1994; Schmitt et al. 2003). The SH left Humerus XV is within the range of recent human values in both absolute SBV and absolute bone weight although, relative to bone size and body size, continues to show a difference in both parameters.

Another argument in favor of the systemic origin of skeletal differences is that hypertrophy of the cortical bone appears relatively early in ontogeny (Ruff et al. 1994; Cowgill, 2010), and is present in very young Neandertal individuals such as Kiik-Koba (5–12 months; Vlcek, 1973), Dederiyeh 1 (2 years; Sawada et al. 2004), La Ferrassie 6 (3–5 years; Heim, 1982) and Cova Negra (about 5 years; Arsuaga et al. 2007). On the contrary, Cowgill (2010) found that the Upper Paleolithic children from Lagar Velho 1 and Yamashita-cho 1 display relatively thin cortical bone, and conclude that differences at the population level appear to be systemic. Moreover, thick cortical bone is also found at an early developmental age at least in early Pleistocene hominins from Europe (Bermúdez de Castro et al. 2012), as well as in the sub-adults from the same Middle Pleistocene SH site whose adults are reported here (García-González et al. 2016).

With these findings at hand, it is difficult for arguments based solely on mechanical loading to explain population differences in diaphyseal robusticity before the age of 1 year (Cowgill, 2010). The appearance of relatively high skeletal robusticity in very young individuals, surely well before they experienced high activity levels, seems to be a strong argument supporting a substantial genetic component for this trait. In addition, we must also consider that *Homo ergaster* (Dean & Smith, 2009; Dean & Liversidge, 2015) and *Homo neanderthalensis* (Guatelli-Steinberg, 2009; Smith et al. 2010) had an overall accelerated growth rate, and that at least Neandertal children were ahead of modern children in growth and development and were larger than recent humans of the same developmental age (Smith, 1991; Churchill, 1998), which heightened their robusticity. Although not yet resolved using dental remains, we can at least say that the skeletal developmental pattern of *Homo antecessor* and the SH hominins coincides consistently with that of the more advanced individuals of different samples from *H. sapiens* (García-González et al. 2009, 2016). Thus, we agree with previous claims that Neandertal children (and we believe the children from the SH site too) started out larger than their modern counterparts and stayed larger than recent children. Natural selection would have favored large, robust infants that, in terms of skeletal

robusticity, started with a significant advantage in bone mass compared with *H. sapiens*.

The possible presence of thickened cortical bone (and more bone volume) throughout all bones of the skeleton and in all SH individuals would be another argument to support a systemic origin for this feature. At present, this is best documented in adult (Rodriguez et al. 2016; Rodríguez et al. 2018) and sub-adult (García-González et al. 2016) long bones and the cranial vault (Arsuaga et al. 1997). The significance of cranial vault thickness in archaic humans has been debated (Gauld, 1996; Lieberman, 1996). Given that it may have little effect on the performance of the cranium in response to loading (Pearson & Lieberman, 2004), it is either indicative of a generalized systemic larger bone volume throughout the skeleton, or is a by-product caused by physical activity. Interestingly, allometric patterns of cranial bone thickness in Asian *Homo erectus* suggest that the published body weight estimates greatly underestimate actual mean body size for members of this species. Its cranial bone thickness to body mass relationship is dissimilar to that displayed by all other catarrhine taxa, including other hominin species (Gauld, 1996). In this sense, the dentine in Neandertals is relatively thicker than in modern humans (Smith et al. 2012). Unlike enamel, dentin and bone have the same embryological (mesoderm) origin, that is, they are basically the same type of tissue. If a greater quantity of bone is a systemic (mainly genetic) trait, the formative and regulatory processes affecting bone formation could quite likely also affect dentin.

In our view, the high skeletal robusticity of the SH sample, including larger bone volume and skeletal weight, is part of their adaptive body type (size and shape; Arsuaga et al. 2015) selected for over the course of the Pleistocene to support different mechanical and lifestyle demands (which were clearly more physically rigorous in Pleistocene hominins than in many modern human samples). But this biotype is constructed under a tight genetic control, including control over bone formative and regulatory processes.

Whether and to what extent changes in skeletal weight during our evolutionary history have affected body mass is still not completely evaluated, but the differences in 'body mass' and 'daily energy expenditure' estimates using the different approaches in Table 6 are an excellent indication of how much bone volume should be taken into account in our calculations. Further comparisons of the SH adult and sub-adult bones with additional fossil and recent human groups should lead to a more refined conclusion regarding the differences in bone volume and skeletal mass with recent humans. However, the differences found here are large enough to suggest some paleobiological implications. If finally demonstrated, the larger skeletal bone volume and skeletal weigh of the SH humans (and maybe all archaic humans) is a variable that paleoanthropologists could consider in their research, given the relevant interest of estimating the body mass of fossil human specimens in paleobiological studies.

Acknowledgements

The author thank Leslie Aiello for her constructive criticism on an early version of this study. The authors have benefitted from fruitful discussions with their colleagues from the Centro UCM-ISCIII sobre Evolución y Comportamiento Humanos of Madrid and the Laboratorio de Evolución Humana at the University of Burgos. Thanks also to the anonymous reviewers of the manuscript for their valuable comments. This research was supported by the Ministerio de Educación y Ciencia Project N° CGL2012 38434-C03-01 and CGL 2015-65387-C3-2-P (MINECO-FEDER), and by the Junta de Castilla y León Project N° BU005A09. Fieldwork at the Atapuerca sites is funded by the Junta de Castilla y León and the Fundación Atapuerca. The authors declare no conflicts of interest.

Authors' contributions

Concept/design: J.M.C., L.R.; acquisition of data: L.R., R.G.G., J.M.C.; data analysis/interpretation: J.M.C., L.R., R.G.G., R.M.Q., J.L.A.; writing the paper: J.M.C., L.R., R.M.Q.; drafting and revision of the manuscript: J.M.C., L.R., R.G.G., R.M.Q., J.L.A.; approval of the article: J.M.C., L.R., R.G.G., R.M.Q., J.L.A.

References

Aiello LC (1992) Allometry and the analysis of the size and shape in human evolution. *J Hum Evol* **22**, 127–147.

Aiello LC, Key C (2002) Energetic consequences of being a Homo erectus female. *Am J Hum Biol* **14**, 551–565.

Alexander RM (1992) A model of bipedal locomotion on compliant legs. *Philos Trans R Soc Lond B Biol Sci* **338**, 189–198.

Arsuaga JL, Martinez I, Gracia A, et al. (1997) The Sima de los Huesos crania (Sierra de Atapuerca, Spain). A comparative study. *J Hum Evol* **33**, 219–281.

Arsuaga JL, Lorenzo C, Carretero JM, et al. (1999) A complete human pelvis from the Middle Pleistocene of Spain. *Nature* **399**, 255–258.

Arsuaga JL, Villaverde V, Quam R, et al. (2007) New Neandertal remains from Cova Negra (Valencia, Spain). *J Hum Evol* **52**, 31–58.

Arsuaga JL, Martínez I, Arnold LJ, et al. (2014) Neandertal roots: cranial and chronological evidence from Sima de los Huesos. *Science* **344**, 1358–1363.

Arsuaga JL, Carretero JM, Lorenzo C, et al. (2015) Postcranial morphology of the middle Pleistocene humans from Sima de los Huesos, Spain. *Proc Natl Acad Sci USA* **112**, 11 524–11 529.

Auerbach BM, Ruff CB (2004) Human body mass estimation: a comparison of "Morphometric" and "Mechanical" methods. *Am J Phys Anthropol* **125**, 331–342.

Baker PT, Newman RS (1957) The use of bone weight for human determination. *Am J Phys Anthropol* **15**, 601–618.

Baldock PA, Eisman JA (2004) Genetic determinants of bone mass. *Curr Opin Rheumatol* **16**, 450–456.

Bermúdez de Castro J, Carretero JM, García-González R, et al. (2012) Early pleistocene human humeri from the Gran Dolina

TD6 site (Sierra de atapuerca, Spain). *Am J Phys Antropol* **147**, 604–617.

Blain HA, Bailon S, Cuenca-Bescós G, et al. (2009) Long-term climate record inferred from early-middle Pleistocene amphibian and squamate reptile assemblages at the Gran Dolina Cave, Atapuerca, Spain. *J Hum Evol* **56**, 55–65.

Bonmati A, Gómez-Olivencia A, Arsuaga JL, et al. (2010) Lower back and pelvis from an aged human individual from the Sima de los Huesos site (Spain). *Proc Natl Acad Sci USA* **107**, 18 386–18 391.

Carretero JM, Rodríguez L, García-González R, et al. (2012) Stature estimation from complete long bones in the Middle Pleistocene humans from the Sima de los Huesos, Sierra de Atapuerca (Spain). *J Hum Evol* **62**, 242–256.

Churchill SE (1996) Particulate versus integrated evolution of the upper body in Late Pleistocene humans: a test of two models. *Am J Phys Antropol* **100**, 559–583.

Churchill SE (1998) Cold adaptation, heterochrony and Neandertals. *Evol Anthropol* **7**, 46–60.

Ciarelli MJ, Goldstein SA, Kuhn JL, et al. (1991) Evaluation of orthogonal mechanical properties and density of human trabecular bone from the major metaphyseal regions with materials testing and computed tomography. *J Orthop Res* **9**, 674–682.

Clarys JP, Martin AD, Marfell-Jones MJ, et al. (1999) Human body composition; a review of adult dissection data. *Am J Hum Biol* **11**, 167–174.

Cowgill LW (2010) The ontogeny of Holocene and Late Pleistocene human postcranial strength. *Am J Phys Anthropol* **141**, 16–37.

Currey JD (1984) Effects of differences in mineralization on the mechanical properties of bone. *Philos Trans R Soc Lond B Biol Sci* **304**(1121), 509–518.

Currey JD (2002) *Bones: Structure and Mechanics*. Princeton: Princeton University Press.

Daly RM, Saxon L, Turner CH, et al. (2004) The relationship between muscle size and bone geometry during growth and in response to exercise. *Bone* **34**, 281–287.

Damuth J, MacFadden BJ (1990) *Body Size in Mammalian Paleobiology: Estimation and Biological Implications*. Cambridge: Cambridge University Press.

Dean MC, Liversidge HM (2015) Age estimation in fossil hominins: comparing dental development in early Homo with modern humans. *Ann Hum Biol* **42**(4), 415–429.

Dean MC, Smith BH (2009) Growth and development of the Nariokotome Youth, KNM-WT 15000. In: *The First Humans–Origin and Early Evolution of the Genus Homo. Vertebrate Paleobiology and Paleoanthropology* (eds Grine FE, Fleagle JG, Leakey RE), pp. 101–120. Dordrecht, Netherlands: Springer.

Forwood MR, Burr DB (1993) Physical activity and bone mass: exercises in futility? *Bone Miner* **21**, 89–112.

Froehle AW, Churchill SE (2009) Energetic competition between Neandertals and anatomically modern humans. *PaleoAnthropology* **2009**, 96–116.

García-González R, Carretero JM, Rodríguez L, et al. (2009) Étude analytique d'une clavicule complète de subadulte d'Homo antecessor (site Gran Dolina, Sierra d'Atapuerca, Burgos, Espagne). *L'Anthropologie* **113**, 222–232.

García-González R, Rodríguez L, Carretero JM, et al. (2016) The ontogeny of femoral strength in Middle Pleistocene humans from Sima de los Huesos (Atapuerca, Spain). *Proceedings of the European Society for the Study of Human Evolution* 5, Alcalá de Henares (Madrid, Spain), p. 103.

Gauld SC (1996) Allometric patterns of cranial bone thickness in fossil hominids. *Am J Phys Anthropol* **100**, 411–426.

Grine FE, Jungers WL, Tobias PV, et al. (1995) Fossil Homo femur from berg aukas, Northern Namibia. *Am J Phys Anthropol* **97**, 151–185.

Guatelli-Steinberg D (2009) Recent studies of dental development in Neandertals: implications for Neandertal life histories. *Evol Anthropol* **18**, 9–20.

Hazelwood SJ, Martin BB, Rashid MM, et al. (2001) A mechanistic model for internal bone remodeling and turnover of iliac bone: implications for mechanisms of bone loss. *J Biomech* **34**, 299–308.

Heim JL (1982) *Les Enfants Ne'andertaliens de La Ferrassie*. Paris: Masson.

Hildebrand M, Hurley JP (1985) Energy of the oscillating legs of a fast-moving cheetah, pronghorn, jackrabbit, and elephant. *J Morphol* **184**, 23–31.

Holt BM (2003) Mobility in upper paleolithic and mesolithic europe: Evidence from the lower limb. *Am J Phys Anthropol* **122**, 200–215.

Ingalls NW (1931) Observations on bone weights. *Am J Anat* **48**, 45–98.

Judex S, Garman R, Squire M, et al. (2004) Genetically based influences on the site-specific regulation of trabecular and cortical bone morphology. *J Bone Miner Res* **19**, 600–606.

Jungers WL (1988) New estimates of body size in australopithecines. In: *Evolutionary History of the "Robust" Australopithecines* (ed. Grine FE), pp. 115–125. New York, NY: Aldine de Gruyter.

Larsen CS, Ruff CB, Kelly RL (1995) Structural analysis if the Stillwater postcranial human remains: Behavioral implications of articular joint pathology and long bone diaphyseal morphology. In: CS Larsen & RL Kelly (Eds.), *Bioarchaeology of Stillwater Marsch* (Vol. 77). New York: American Museum of Natural History.

Lieberman D (1996) How and why humans grow thin skulls: experimental evidence for systemic cortical robusticity. *Am J Phys Anthropol* **101**, 217–236.

Lorenzo C, Carretero JM, Arsuaga JL, et al. (1998) Intrapopulational body size variation and cranial capacity variation in middle pleistocene humans: the sima de los huesos sample (Sierra de Atapuerca, Spain). *Am J Phys Anthropol* **106**, 19–33.

Lowrance EW, Latimer HB (1957) Weights and linear measurements of 105 human skeletons from Asia. *Am J Anat* **101**, 445–459.

Maimon L, Sultan C (2011) Effects of physical activity in bone remodeling. *Metabolism* **60**, 373–388.

Malina R, Bouchard C (1991) *Growth, Maturation and Physical Activity*. Champaign, IL: Human Kinetic Books.

Marchi D (2008) Relationship between lower limb cross-sectional geometry and mobility: The case of a Neolithic sample from Italy. *Am. J. Phys. Anthropol* **137**, 188–200.

Martin RB (2003) Technical Note. Fatigue damage, remodeling, and the minimization of skeletal weight. *J Theor Biol* **220**, 271–276.

McGuigan FE, Murray L, Gallagher A, et al. (2002) Genetic and environmental determinants of peak bone mass in young men and women. *J Bone Miner Res* **17**, 1273–1279.

McHenry HM (1992) Body size and proportions in early hominids. *Am J Phys Anthropol* **87**, 407–431.

Merz AL, Trotter M, Peterson RR (1956) Estimation of skeletal weight in the living. *Am J Phys Anthropol* **14**, 589–609.

Moisio KC, Hurwitz DE, Sumner DR (2004) Dynamic loads are determinants of peak bone mass. *J Orthop Res* **22**, 329–345.

Oliveira RCG, Leles CR, Normanha LM, et al. (2008) Assessments of trabecular bone density at implant sites on CT images. *Oral Surg Oral Med Oral Pathol Oral Radiol Endod* **105**, 231–238.

Pearson OM, Lieberman DE (2004) The aging of Wolff's "law": ontogeny and responses to mechanical loading in cortical bone. *Am J Phys Anthropol* **125**, 63–99.

Peck JJ, Stout SD (2007) Intraskeletal variability in bone mass. *Am J Phys Antropol* **132**, 89–97.

Ponce de Leon MS, Golovanova L, Doronichev V, et al. (2008) Neanderthal brain size at birth provides insights into the evolution of human life history. *Proc Natl Acad Sci USA* **105**, 13 764–13 768.

Rodriguez L, Carretero JM, Garcia-Gonzalez R, et al. (2016) Fossil hominin radii from the Sima de los Huesos Middle Pleistocene site (Sierra de Atapuerca, Spain). *J Hum Evol* **90**, 55–73.

Rodríguez L, Carretero JM, García-González R, et al. (2018) Cross-sectional properties of the lower limb long bones in the Middle Pleistocene Sima de los Huesos sample (Sierra de Atapuerca, Spain). *J Hum Evol* **117**, 1–12.

Rubin CT, Lanyon LE (1984) Regulation of bone-formation by applied dynamic loads. *J Bone Joint Surg* **66**, 397–402.

Ruff CB (2003) Growth in bone strength, body size, and muscle size in a juvenile longitudinal sample. *Bone* **33**, 317–329.

Ruff CB, Niskanen M (2018) Introduction to special issue: body mass estimation–methodological issues and fossil applications. *J Hum Evol* **115**, 1–7.

Ruff CB, Scott WW, Liu A (1991) Articular and diaphyseal remodeling of the proximal femur with changes in body mass in adults. *Am J Phys Anthropol* **86**, 397–413.

Ruff CB, Trinkaus E, Walker A, et al. (1993) Postcranial robusticity in *Homo*. I: Temporal trends and mechanical interpretation. *Am J Phys Anthropol* **91**, 21–53.

Ruff CB, Walker A, Trinkaus E (1994) Postcranial robusticity in Homo. III: Ontogeny. *Am J Phys Antropol* **93**, 35–54.

Ruff CB, Trinkaus E, Holliday TW (1997) Body mass and encephalization in Pleistocene Homo. *Nature* **387**, 173–176.

Ruff CB, Niskanen M, Junno J, et al. (2005) Body mass prediction from stature and bi-iliac breadth in two high latitude populations, with application to earlier higher latitude humans. *J Hum Evol* **48**, 318–392.

Ruff CB, Holt B, Trinkaus E (2006) Who's afraid of the big bad Wolff?: "Wolff's law" and bone functional adaptation. *Am J Phys Anthropol* **129**, 484–498.

Sawada J, Kondo O, Nara T, et al. (2004) Bone histomorphology of the Dederiyeh Neanderthal child. *Anthropol Sci* **112**(3), 247–256.

Schmitt D, Churchill SE, Hylander WL (2003) Experimental evidence concerning spear use in Neandertals and early modern humans. *J Archaeol Sci* **30**(1), 103–114.

Seeman E (1997) From density to structure: growing up and growing old on the surfaces of bone. *J Bone Miner Res* **12**, 509–521.

Shackelford LL (2007) Regional variation in the postcranial robusticity of late Upper Paleolithic humans. *Am J Phys Anthropol* **133**, 655–668.

Shephard RJ (1991) *Body Composition in Biological Anthropology*. Cambridge: Cambridge University Press.

Silva AM, Crubezy E, Cunha E (2008) Bone weight: new reference values based on a modern Portuguese identified skeletal collection. *Int J Osteoarchaeol* **19**, 628–641.

Smith FH (1991) The Neandertals: evolutionary dead ends or ancestors of modern people? *J Anthropol Res* **47**, 219–238.

Smith T, Tafforeau P, Reid D, et al. (2010) Dental evidence for ontogenetic differences between modern humans and Neanderthals. *Proc Natl Acad Sci USA* **107**(49), 20 923–20 928.

Smith TM, Olejniczak AJ, Zermeno JP, et al. (2012) Variation in enamel thickness within the genus Homo. *J Hum Evol* **62**, 395–411.

Sokal RR, Rohlf FJ (1979) *Biometria : principios y métodos estadísticos en la investigación biológica*. Madrid: Blume Ediciones.

Sorensen MV, Leonard WR (2001) Neandertal energetics and foraging efficiency. *J Hum Evol* **40**, 483–495.

Sparacello VS, Marchi D (2008) Mobility and subsistence economy: a diachronic comparison between two groups settled in the same geographical area (Liguria, Italy). *Am. J. Phys. Anthropol* **136**, 485–495.

Spoor CF, Zonneveld FW, Macho GA (1993) Linear measurements of cortical bone and dental enamel by computed tomography: applications and problems. *Am J Phys Anthropol* **91**, 469–484.

Stock JT (2006) Hunter-Gatherer postcranial robusticity relative to patterns of mobility, climatic adaptation and selection for tissue economy. *Am J Phys Anthropol* **131**, 194–204.

Trinkaus E, Ruff CB (2012) Femoral and tibial diaphyseal cross-sectional geometry in pleistocene Homo. *PaleoAnthropology* **2012**, 13–62.

Trinkaus E, Churchill SE, Ruff CB (1994) Postcranial robusticity in Homo. II: Humeral bilateral asymmetry and bone plasticity. *Am J Phys Anthropol* **93**(1), 1–34.

Trotter M (1954) A preliminary study of estimation of weight of the skeleton. *Am J Phys Anthropol* **12**, 537–551.

Vlcek E (1973) Postcranial skeleton of a Neandertal child from Kiik-Koba, U.S.S.R. *J Hum Evol* **2**, 537–544.

Warton DI, Wright IJ, Falster DS, et al. (2006) Bivariate line-fitting methods for allometry. *Biol Rev* **81**, 259–291.

White TD, Folkens PA (2000) *Human Osteology (2nd edn)*. San Diego, California: Academic Press.

Yerges LM, Klei L, Cauley JA, et al. (2010) Candidate gene analysis of femoral neck trabecular and cortical volumetric bone mineral density in older men. *J Bone Miner Res* **25**, 330–338.

Zilhman A, Bolter D (2015) Body composition in Pan paniscus compared with *Homo sapiens* has implications for changes during human evolution. *Proc Natl Acad Sci USA* **112**, 7466–7471.